Synthetic Metals, 5 (1983) 205 - 216

SUPERCONDUCTING PROPERTIES OF METALLIC HETEROSTRUCTURES

IVAN K. SCHULLER

Argonne National Laboratory, Argonne, IL 60439 (U.S.A.)

CHARLES M. FALCO

Departments of Physics and Optical Sciences and Arizona Research Laboratories, University of Arizona, Tucson, AZ 85721 (U.S.A.)

Summary

We review our recent results on the superconducting properties of artificially prepared metallic heterostructures. Our sputtering system used to prepare these materials is described in detail along with a calculation of the thermalization of sputtered atoms. The structure of Nb/Cu and Nb/Ti heterostructures is discussed, as are T_c, energy gap, and phonon frequency measurements.

Introduction

Recently we have prepared a new class of artificially layered metals termed Layered Ultrathin Coherent Structure (LUCS) [1, 2]. Some of the physical properties of LUCS have been discussed in other publications [1, 3 - 7]. Here we review our technique for preparing LUCS as well as describing the superconducting properties of Nb/Cu and Nb/Ti LUCS. Also reviewed is a calculation of the energy distribution of the sputtered particles arriving at the substrate. This calculation indicates an important advantage sputtering has over evaporation for such artificially layered materials, especially for refractory metals.

Sample growth

Two separated and highly baffled, high-rate magnetron sputtering guns are in a diffusion pumped high vacuum system (base pressure $\sim 8 \times 10^{-8}$ Torr). Deposition rates of 10 - 200 Å/s at the substrate are typically used. We find the rates from the guns to be very stable and reproducible run-to-run, so that active feedback control is not necessary. The rates are determined by the total power applied to the guns. The rate at fixed power is weakly dependent on argon pressure with an effect of less than 0.5%/mTorr in the typical region of operation. Pressure is regulated to better than 0.1

0379-6779/83/0000-0000/$03.00

mTorr. Although results will not be discussed here, this system can also be used for reactive sputtering by introducing a partial pressure of suitable gas. Pressure is measured both by an ionization gauge and by a capacitance transducer. The rates are monitored during deposition using two quartz crystal oscillators.

Single crystal 90° or 0° oriented sapphire, mica, MgO, etc., substrates are held on a rotating platform whose temperature is controlled using a non-contact temperature sensor and quartz lamp heater in a feedback configuration. This allows the substrate temperature to be varied from room temperature to approximately 400 °C to an accuracy of ±2 °C. This temperature control is important, as can be seen from Fig. 1 where we show X-ray diffraction data from a series of Ag samples grown on mica at various temperatures [8] (in collaboration with M. Khan). Although the dominant feature for samples grown at room temperature is from the (111) texture, there is a significant fraction of (200) present. The (200) line disappears when samples are grown at higher temperatures. From transmission Laue measurements (not shown here), the Ag is found to grow epitaxially as a (111) oriented single crystal only at the highest temperature of 270 °C. Below this temperature, the Laue measurements show both crystalline spots and polycrystalline rings.

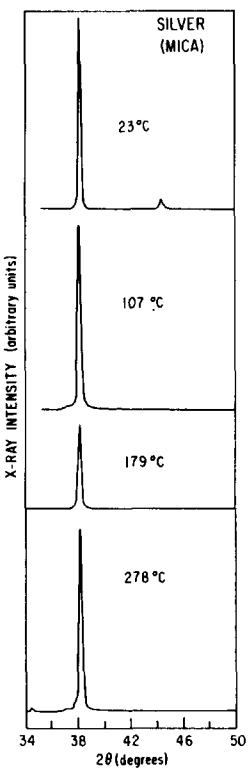

Fig. 1. Bragg θ - 2θ X-ray diffraction data from series of Ag samples grown on cleaved mica substrates.

Radiation from the rather large substrate platform is the dominant heat less mechanism, and presently limits the upper substrate temperature in our system to approximately 400 °C. The platform position can be altered to vary the distance of the substrates from the guns over the range 0.5 - 30 cm. As will be discussed below, this distance can also be an important parameter for obtaining epitaxial growth.

One advantage of sputtering over standard evaporation techniques is that control of both the sputtering pressure and of the target/substrate distance allows control of the energy distribution of particles arriving at the substrate. This can easily be understood since typical sputtering pressures are in the range 1 - 20 mTorr. This corresponds to mean free paths of from a fraction of a centimeter to many centimeters. Thus we can adjust the parameters of our system (pressure and distance) to cause the sputtered particles to arrive either with no energy loss or with a large energy loss due to many collisions with the Ar gas. To understand this effect more exactly, we have calculated the energy distribution of sputtered Nb and Cu particles arriving at the substrate for various target to substrate distances [9]. Results for the case of Nb are shown in Fig. 2. Notice that the higher the sputtering pressure the more rapidly the final distribution approaches the thermal Maxwell–Boltzman distribution of the sputtering gas. A comparison (Fig. 3) of the

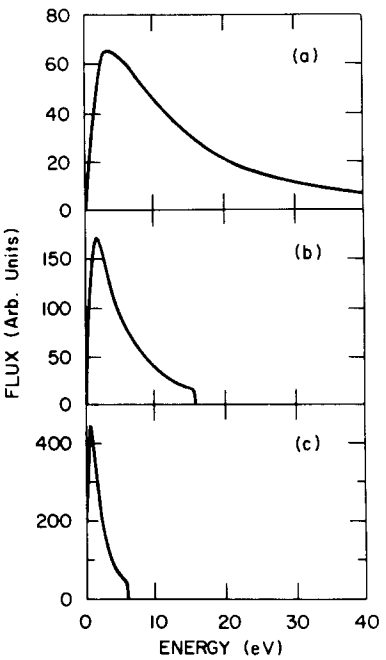

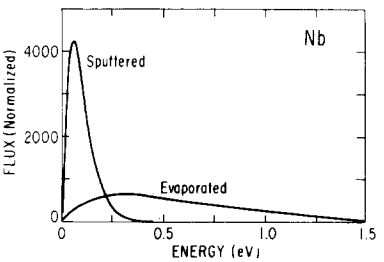

Fig. 2. Niobium energy distribution calculated according to the model described in ref. 9 for various distances traveled from the target with Ar gas pressure 10 mTorr. Distances are (a) 0 cm, (b) 3 cm, (c) 6 cm.

Fig. 3. Calculated final energy distributions for sputtered and thermally evaporated Nb.

energy distribution of sputtered and evaporated Nb (for identical rates at the substrate) shows the sputtered distribution to be sharper, with a peak energy lower than that of evaporated Nb. This effect is most pronounced for refractory materials.

It is important for the temperature of the substrate as well as the deposition rates to be high enough to promote epitaxy [10]. At the same time care should be taken that the energy of the particles arriving at the substrate is low enough to avoid disrupting the already formed layers. This is easily accomplished using sputtering since the energy distribution and peak energy can be manipulated by changing sputtering pressure and substrate to target distance.

Structural measurements

Determination of the composition as a function of depth into the sample with resolution at a scale down to the atomic level is highly desirable so that the nature and quality of the interface between layers can be studied. Although there are several surface analysis probes available with depth resolution of roughly the atomic scale (*e.g.*, Auger and Ion Scattering Spectroscopy (ISS)), there are difficulties in applying them to this problem. The difficulty with ion mill Auger spectroscopy for this purpose is two-fold. The escape depth for the Auger electrons is energy dependent, but even in the most favorable case is ~20 Å. Therefore, the Auger signal is only indicative of the chemical composition averaged over at least a 20 Å depth, *i.e.*, approximately 8 - 10 atomic layers. An additional problem is that the process of ion milling causes significant intermixing of the layers as well as cratering which destroys the layered structure.

In order to obviate the finite escape depth problem inherent in the Auger measurements, ion mill ISS measurements have been performed. For the first layer of a 65 Å-layer-thickness Nb/Cu sample, we observe essentially 100% composition modulation; however, intermixing problems caused by the ion milling can clearly be seen to distort the results for subsequent layers. The chemical composition of these materials is shown by these measurements to be modulated, but ion milling techniques are not useful for layer thicknesses below ~40 Å.

We have performed both standard X-ray scattering and Laue X-ray scattering on both the Nb/Cu and Nb/Ti discussed here, as well as on Nb/Ni and Ni/Ag samples, to study the crystal structure. Since, for the case of θ - 2θ scans the X-ray momentum transfer is perpendicular to the layers, this measurement is only sensitive to structural changes perpendicular to the layers. A one dimensional model calculation assuming 100% composition modulation and equal layer thicknesses indicates that characteristic peaks should arise due to scattering by the superlattice planes [2]. The layer thickness (d) is given by the simple formula

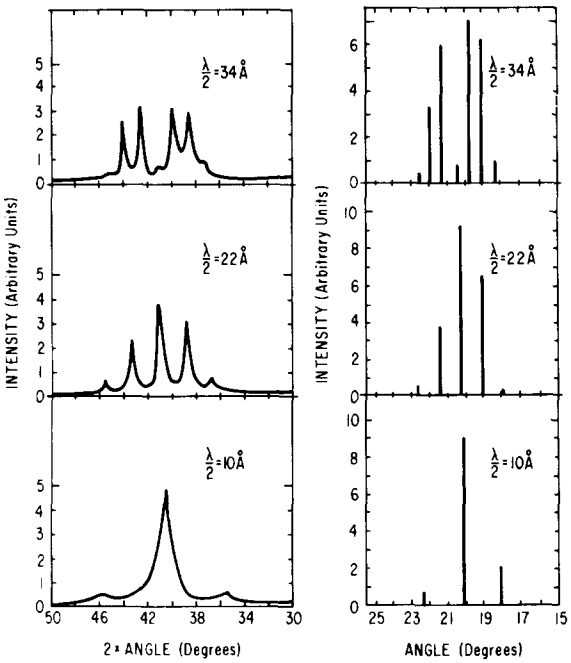

Fig. 4. Measured and calculated θ - 2θ Bragg X-ray diffraction patterns for several Nb/Cu samples of different layer thickness ($d = \lambda/2$).

$$d = \frac{\lambda_x}{\sin\theta_i - \sin\theta_{i+1}} \tag{1}$$

where λ_x is the X-ray wavelength and i and $i + 1$ refer to adjacent diffraction peaks. The measured and calculated X-ray intensities *vs.* 2θ for a series of Nb/Cu samples are shown in Fig. 4. The existence of a large number of superlattice reflections implies that the position of atomic planes perpendicular to the layers is correlated. As in any anisotropic system, several coherence lengths can be defined. In particular, the X-ray measurement described above gives a lower limit on the coherence of the Nb/Cu superlattice in the z direction (perpendicular to the layers) of ~200 Å for superlattice wavelengths in the range 20 - 70 Å. For superlattices outside this range, the superlattice X-ray peaks merge into a central peak or peaks.

For the Nb/Ti samples in the layer thickness range 7 Å $< d <$ 70 Å it was found that Nb (bcc) and Ti (hcp) deposit in a (110) and (0001) texture respectively [11]. The interplane spacing of Nb (110) is 2.334 Å. For Ti the (0001) hcp spacing is 2.3422 Å and the metastable (110) bcc spacing is 2.355 Å. Thus a θ - 2θ diffractometer scan about the normal to the substrate provides insufficient information to uniquely characterize the structure in the Ti-rich regions of a given layer.

Transmission Laue photographs were taken on a sample which was stripped off the sapphire substrate, to obtain further information. The ob-

servation of several rings rather than spots implies the presence of a texture rather than epitaxy, with the grain size of the crystallites small on the X-ray beam diameter scale (~0.5 mm). Three of these rings correspond to the (211), (310) and (011) (and equivalent) planes of the bcc structure with a (110) plane normal. A fourth ring could not be indexed with a plane of the bcc or hcp structures assuming (110) or (0001) plane normals, respectively (the diffractometer scan showing the presence of no other textures). This ring does index with a (111) plane of the fcc structure assuming a (111) plane normal. A diffractometer scan, with the film rotated to place the other (111) plane normal to the θ - 2θ scan axis, yielded a plane spacing consistent with an fcc structure having the same interatomic distance (2.342 Å) as the Ti hcp structure. Since it is well known [10] that many of the bcc transition metals adopt fcc structures in thin films we presumably have some fcc Ti. A diffractometer scan with the film rotated such that the (011) plane of the hcp structure was normal to the scan axis showed the presence of a small amount of hcp Ti. The above structural studies indicate that most of the Ti is in the bcc phase.

Superconducting transition temperatures

(a) Nb/Cu

Inductive and resistive T_c measurements on Nb/Cu were made, with agreement of the two techniques to within a few mK [3]. Each sample showed one sharp transition. For thick layers of Nb/Cu a T_c of 8.91 K, characteristic of pure Nb, is found, with T_c decreasing as the layer thickness decreases until it saturates at ~2.8 K for thin layers.

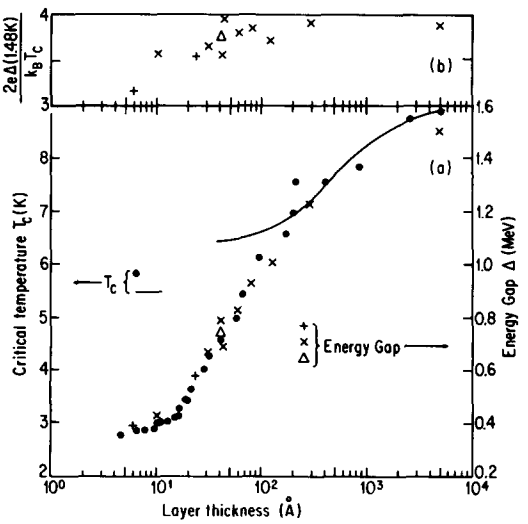

Fig. 5. (a) Critical temperature and energy gap *vs.* layer thickness for a series of Nb/Cu samples. As discussed in the text, energy gaps determined using several different Al overlayer thicknesses: +, 80 Å; ×, 50 Å; △, 20 Å. (b) $2\Delta/kT_c$ *vs.* layer thickness.

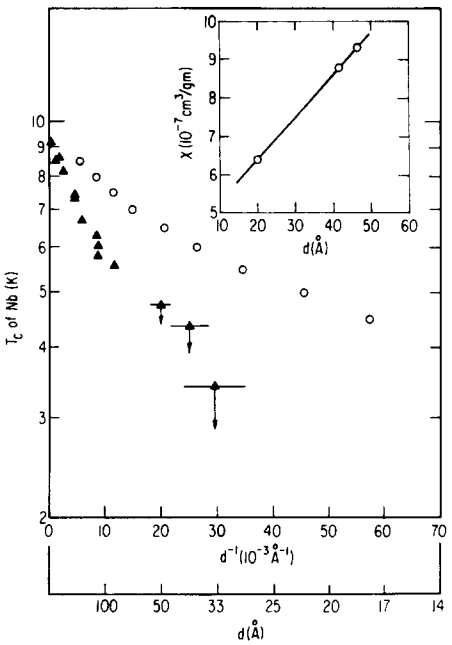

Fig. 6. Intrinsic T_c of isolated thin Nb layer as inferred from fit to de Gennes–Werthamer theory to our Nb/Cu heterostructure data. △, data of Wolf *et al.* on single Nb thin films.

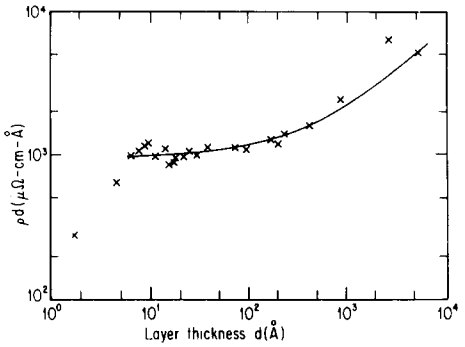

Fig. 7. Measured electrical resistivity at 50 K times layer thickness *vs.* layer thickness for a series of Nb/Cu samples. Solid line provided as a guide to the eye is a straight line on a linear plot.

We used the de Gennes–Werthamer (dGW) theory of the proximity effect to analyze these data [13 - 15]. The solid line in Fig. 5 is a none-adjustable parameter fit of the dGW theory to our data. Deviations between theory and experiment begin to occur where d is becoming comparable with the superconducting coherence length ξ. However, it has been shown that the dGW model is still applicable for $d < \xi$ [15]. Thus our results suggest that the properties of very thin layers of Nb are different from the bulk values assumed for calculating the solid curve in Fig. 5. Assuming the dGW model to be applicable for $d < \xi$, and using the T_c of niobium as an adjustable parameter for $d < 300$ Å allows us to extract the T_c of niobium as a function of film thickness. This result, shown in Fig. 6, is compared with that of Wolf *et al.* [16], where they measured T_c's of single evaporated films of Nb of various thicknesses. The reduced T_c of their thin films, Wolf *et al.* conjectured, was due to contamination of the surface layer; this becomes increasingly important as the films are made thinner. Ion mill Auger and ion mill ISS studies on our layered samples (total thickness always ~1 μm) show that we have well-separated layers with clean interfaces and negligible contamination. Our data then imply that the Nb T_c decreases with decreasing layer thickness down to at least 17 Å. Since, as shown by Fig. 7, the resistivity of

our samples increases linearly with decreasing layer thickness down to at least 10 Å, and susceptibility measurements [19] show a decrease in χ as a function of layer thicknesses, these facts are in qualitative agreement with the idea that the density of states is affected by the decrease in the mean free path [17, 18].

(b) Nb/Ti

T_c measurements were performed on all Nb/Ti samples using an a.c. mutual inductance bridge with the oscillating field applied parallel to the film [11]. In addition, the transition was studied resistively in four samples with agreement found with the inductive measurements. Figure 8 shows the inductively measured transition temperatures for the samples having layer thicknesses between 7 and 70 Å. The dominant transition observed in the inductance signal is that occurring at the lower temperature. However, a weaker transition (at least four times smaller change in signal) was observed at a higher temperature of about 8.3 K in some samples. The fact that this transition does not correlate with the wavelength, and is relatively weak, suggests that it may be due to a small amount of phase separated Nb.

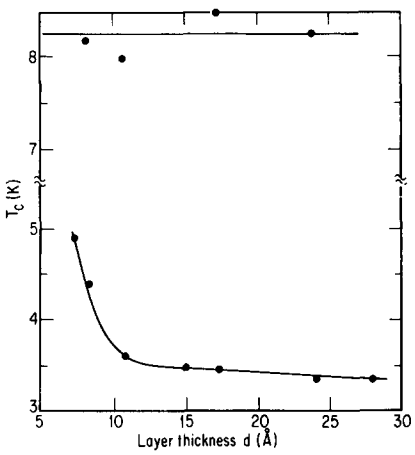

Fig. 8. T_c *vs.* layer thickness for a series of Nb/Ti samples.

The lowering of the dominant transition temperature relative to Nb can be understood as proximity effect averaging between Nb and Ti. The transition temperature of pure Nb in our sputtering unit is 8.9 - 9.2 K (whereas it is 9.2 K in bulk). Similarly prepared films of Ti were not superconducting down to 1.9 K. A transition temperature of ~3.5 K in the modulated structures for layer thicknesses larger than 10 Å implies that either: (i) The majority of the Ti is not in the bcc structure. If this phase were dominant, one would expect at large layer thicknesses a temperature intermediate between the T_c of bcc Nb (9.2 K) and that of bcc Ti (4.0 K). (ii) T_c's of bcc Ti and Nb are suppressed relative to the bulk values. Evidence for this possibility comes from the extensive proximity effect study of the Nb/Cu LUCS

system described above. At very low layer thicknesses of ~10 Å we find an increase in T_c, possibly due to the formation of high T_c ($T_c \cong 10$ K) Nb–Ti alloys at the interfaces of the two materials.

Tunneling studies of Nb/Cu

Tunneling studies were performed on Nb/Cu samples prepared as described above [20]. The only exception is that in order to use a technique pioneered by Wolf *et al.* [21], immediately after the final Nb layer of each multilayer was prepared, the Ar sputtering gas was pumped from the chamber and a thin (20 - 80 Å) aluminum overlayer was evaporated. The total elapsed time between deposition of the final Nb layer and overcoating with the Al overlayer was less than 2 min. The tunneling barrier was then formed by 1 - 2 days oxidation in the laboratory environment. The samples were then placed in another deposition system and counter electrodes (In, Pb or Ag) were evaporated. It should be noted that the many attempts to form samples with a final Cu layer all resulted in shorted junctions. All the data presented here are from junctions which satisfy the generally accepted "Rowell" reliability criteria [22].

The energy gap dependence on layer thickness is essentially the same as the T_c dependence, as can be seen from Fig. 5. Note that these results (as are all our measurements) are independent of the thickness of the Al overlayer. Consequently, as Fig. 5 also shows, the coupling strength ($2\Delta/kT_c$) exhibits little variation, decreasing from ~3.8 for thick layers to slightly less than ~3.5 for thin layers.

Phonons in metals will be directly observable as structure in tunneling d^2V/dI^2 *vs.* V characteristics [23]. The measured second harmonic d^2V/dI^2 *vs.* V curve for a 25 Å Nb/Cu superlattice compared with that of pure Nb is shown in Fig. 9. The three prominent features evident in these curves correspond to the longitudinal acoustic (LA) phonon in aluminum [24] (~37 mV), the longitudinal acoustic (LA) phonon in Nb [25] (~24 mV) and the transverse acoustic (TA) phonon in Nb (~17 mV) [25].

The thin Al overlayer applied to form the tunnel junction serves a valuable role as an internal calibration for the positions and amplitudes of the structures due to phonons in the Nb/Cu. The energy of any aluminum structures such as the LA phonon at ~37 mV should not shift as a function of layer thickness, irrespective of any possible changes in the Nb/Cu phonons. In addition, the peak to peak amplitude of the phonon structure is expected to scale to first order with Δ^2, as has been shown earlier for a variety of systems in a proximity configuration [26, 27]. This result is also observed experimentally, with data spanning an order of magnitude in Δ^2 (and amplitude).

The Nb phonon peaks broaden slightly down to layer thicknesses of ~32 Å but do not shift in energy. This broadening causes the LA phonon to be lost in the background for the thinnest layer sample studied of 10.5 Å.

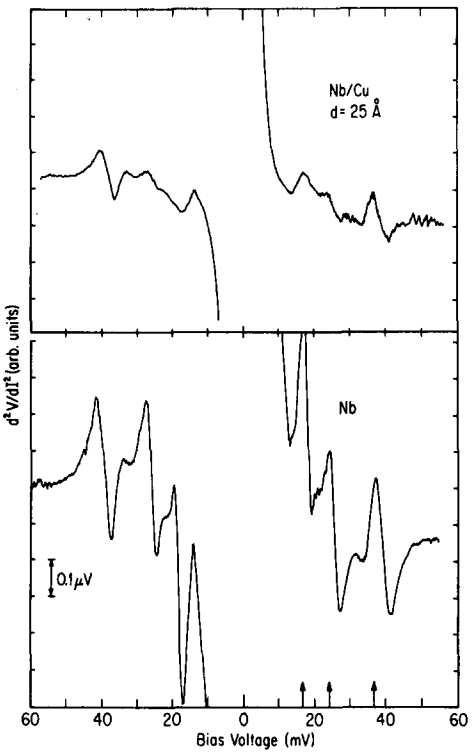

Fig. 9. Second harmonic "d^2/dI^2" *vs.* V curves for a Nb/Cu sample with 25 Å layer thickness and for a pure Nb film.

However, even for this sample there is no evidence for a shift in energy. The observation of bulk-like phonons down to layer thicknesses of 10 Å might seem somewhat surprising at first until it is noted that, since superconductivity mainly samples $2k_F$ phonons, one would not expect to see changes until the thicknesses become comparable to $1/k_F$ (one lattice spacing).

Earlier, using Brillouin light scattering it has been shown [7] that the zone center acoustic phonon in Nb/Cu exhibits a large decrease (20%) in its velocity for layer thicknesses centered around ~10 Å. This result, in conjunction with the tunneling measurements discussed above showing that the zone boundary phonons are pinned at a fixed energy independent of layer thickness, implies that the dispersion relation shows an anomalous "kink" at thicknesses of ~10 Å. Phonon anomalies are exhibited in many high T_c d- and f-band superconductors [28]. It has been shown that T_c is related to these anomalies. Theoretical work has shown that there is a tendency towards the formation of a charge density wave in systems where there is a high density of states at the Fermi surface [29]. The strong electron–phonon coupling in these materials can allow these charge fluctuations to give rise to anomalous phonon dispersion and sometimes to cause structural phase changes. In the Nb/Cu heterostructure system a charge density wave

is artificially imposed on the lattice due to the periodic composition modulation. It is interesting to note that the X-ray line widths start showing considerable broadening around layer thicknesses of $d \sim 10$ Å, indicating that structural changes are taking place below this thickness.

Acknowledgement

We thank our collaborators on various aspects of this research: I. Banerjee, R. T. Kampwirth, J. B. Ketterson, M. Khan, K. Meyer, T. R. Werner, Q. S. Yang and J. Q. Zheng. This work was supported by the U.S. Department of Energy.

References

1 I. K. Schuller and C. M. Falco, in D. U. Gubser, T. L. Francavilla, J. R. Leibowitz and S. A. Wolf (eds.), *Inhomogeneous Superconductors — 1979*, American Institute of Physics, New York, 1980, p. 197.
2 I. K. Schuller, *Phys. Rev. Lett., 44* (1980) 1597.
3 I. Banerjee, Q. S. Yang, C. M. Falco and I. K. Schuller, *Solid State Commun., 41* (1982) 805.
4 C. M. Falco and I. K. Schuller, in G. W. Crabtree and P. D. Vashishta (eds.), *Novel Materials and Techniques in Condensed Matter*, North Holland, New York, 1982.
5 T. R. Werner, I. Banerjee, C. M. Falco and I. K. Schuller, *Phys. Rev. B, 26* (1982) 2224.
6 J. Q. Zheng, C. M. Falco, J. B. Ketterson and I. K. Schuller, *Appl. Phys. Lett., 38* (1981) 424.
7 A. Kueny, M. Grimsditch, K. Miyano, I. Banerjee, C. M. Falco and I. K. Schuller, *Phys. Rev. Lett., 48* (1982) 166.
8 M. Khan, I. K. Schuller and C. M. Falco, *Phys. Status Solidi, (a) 73* (1982) 23.
9 K. Meyer, I. K. Schuller and C. M. Falco, *J. Appl. Phys., 52* (1981) 5803.
10 See, for example, various chapters in J. W. Matthews (ed.), *Epitaxial Growth*, Academic Press, New York, 1975.
11 J. Q. Zheng, J. B. Ketterson, C. M. Falco and I. K. Schuller, *Physica, 108B*, (1981) 945.
12 For the case of Ta see R. B. Marcus and S. Quigley, *Thin Solid Films, 2* (1968) 467.
13 P. G. de Gennes and E. Guyon, *Phys. Lett., 3* (1963) 168.
14 N. R. Werthamer, *Phys. Rev., 132* (1963) 2440.
15 J. J. Hauser, H. C. Theuerer and N. R. Werthamer, *Phys. Rev., 136* (1964) A637.
16 S. A. Wolf, J. J. Kennedy and M. Nisenoff, *J. Vac. Sci. Technol., 13* (1976) 145.
17 J. E. Crow, M. Strongin, R. S. Thompson and O. F. Kammerer, *Phys. Lett., 30A* (1969) 161.
18 C. M. Varma and R. C. Dynes, in D. H. Douglass (ed.), *Superconductivity in d- and f-Band Metals*, Plenum Press, New York, 1976, p. 507.
19 I. Banerjee, *Ph.D. Thesis*, Northwestern University, 1982.
20 Q. S. Yang, C. M. Falco and I. K. Schuller, to be published.
21 E. L. Wolf, J. Zasadzinski, J. W. Osmun and G. B. Arnold, *J. Low-Temp. Phys., 40* (1980) 19.
22 J. M. Rowell, in E. Burnstein (ed.), *Tunneling Phenomena in Solids*, Plenum Press, New York, 1969.
23 See, for example, W. L. McMillan and J. M. Rowell, in R. D. Parks (ed.), *Superconductivity*, Vol. I, Dekker, New York, 1969, p. 561.

24 R. Stedman and G. Nilsson, *Phys. Rev.*, *145* (1966) 492.
25 B. M. Powell, P. Martel and A. D. B. Woods, *Phys. Rev.*, *171* (1968) 727.
26 P. M. Chaikin, G. Arnold and P. K. Hansma, *J. Low-Temp. Phys.*, *26* (1977) 229.
27 B. F. Donovan-Vojtovic, I. K. Schuller and P. M. Chaikin, *Philos. Mag.*, *B39* (1979) 373.
28 See, for example, various articles in D. H. Douglass (ed.), *Superconductivity in d- and f-Band Metals*, Plenum Press, New York, 1976.
29 For a recent review, see S. K. Sinha, in G. K. Horton and H. A. Maradudin (eds.), *Dynamical Properties of Solids*, North Holland, New York, 1980.